International Journal of Environmental Sciences
ISSN: 2229-7359
Vol. 11 No. 4,2025
https://theaspd.com/index.php

Deep Classification Framework for Real-Time Imbalanced Liver Tumor Databases using Combining Probabilistic Segmentation with Ensemble Feature Extraction

N Nanda Prakash[1], V Rajesh[2], Syed Inthiyaz[3], Rahul Joshi[4], Dharmesh Dhabliya[5], Rakesh Ranjan[6], Pramod Ganjewar[7], Shaik Hasane Ahammad[8]

[1,2,3,8]Department of ECE, Koneru Lakshmaiah Education Foundation, Vaddeswaram, Guntur, India, 522302.
[4]CSE Department, Symbiosis Institute of Technology Pune, Symbiosis International (Deemed University) Pune, Maharashtra India.
[5]Professor, Department of Information Technology, Vishwakarma Institute of Technology, Pune, Maharashtra, India.
[6]Department of Computer Science and Engineering, ABES Engineering College, Ghaziabad, UP, India
[7]Department of Computer Engineering, MIT Academy of Engineering, Alandi, Maharashtra, India, 412105, nandaprakashnelaturi@gmail.com, rajesh4444@kluniversity.in, syedinthiyaz@kluniversity.in, rahulj@sitpune.edu.in, dharmeshdhabliya@gmail.com, rakesh.ranjan@abes.ac.in, pdganjewar@mitaoe.ac.in, ahammadklu@gmail.com,

Abstract

As liver tumor image datasets continue to grow, conventional prediction methods encounter difficulties due to significant imbalances between majority and minority classes, as well as the presence of noise. While 3D convolution effectively handles spatial data, it requires substantial GPU resources, whereas 2D convolution is limited in its ability to fully capture the third dimension. Challenges like missing data, noise, and class imbalance adversely affect classification performance, highlighting the critical role of data quality. This study introduces an enhanced ensemble classification model that utilizes k-joint probabilistic segmentation for detecting liver tumors, relying on medical imaging techniques such as CT for feature extraction and segmentation. By incorporating novel filtering and ranking approaches, the model achieves superior recall, precision, and AUC in comparison to current develops.

Keywords: *Deep learning, Imbalance liver image data, support vector machine, ensemble learning model, decision tree.*

1. INTRODUCTION

Liver cancer is one of the fastest-growing causes of cancer deaths worldwide, with delayed diagnosis typically resulting in a poor prognosis. Computed tomography (CT) imaging has an important role in early diagnosis and surgical planning due to its high spatial resolution with a short acquisition time. While CT imaging provides critical detail for surgical planning, it typically requires manual interpretation of scans, making it time-consuming and not standardized, based on inter-observer variability. The level of complexity increases given that tumors can exhibit distinct variations in shape, size, location, and intensity, which makes automated segmentation a major challenge that is currently unresolved in clinical workflows. These challenges highlight a clear need for complex, intelligent systems that can accurately segment and classify liver tumors, without being overburdened by noise and variability, and challenges such as class imbalance. In 2016, liver cancer saw 42,710 new cases reported. Deep learning approaches have demonstrated significant potential in enhancing early detection and treatment efforts. The most common type of liver cancer, hepatocellular carcinoma (HCC), is being identified with greater precision through advanced techniques that improve the accuracy of detecting malignant growths in liver tissues. Medical imaging, particularly CT scans, plays a crucial role in diagnosing liver tumors, although challenges like noise, orientation, and image intensity remain. A novel two-phase tumor segmentation technique focuses on first segmenting the liver, then detecting tumors. The integration of AI and machine vision in medical systems aims to reduce errors and improve care. Despite advancements, liver cancer remains a

significant health threat, highlighting the need for further progress in medical imaging and automated systems [1-3]. The outline of proposed framework is shown in the Fig.1.

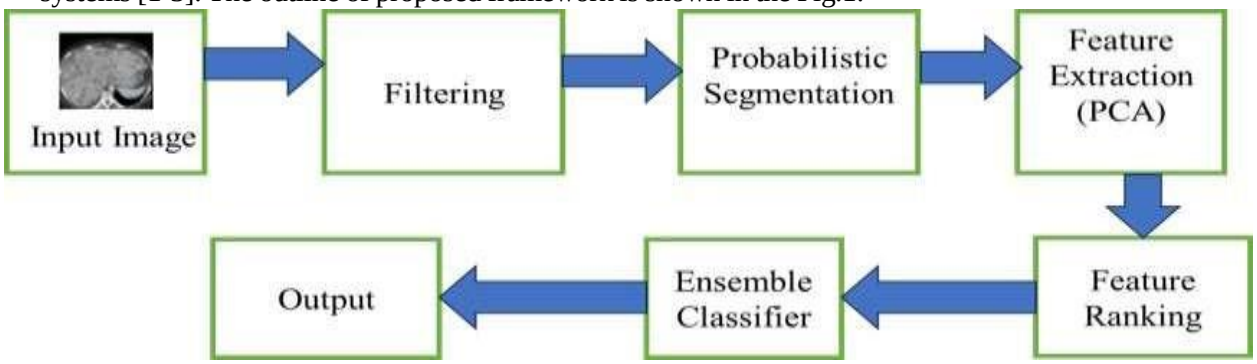

Fig. 1. Outline of Proposed Framework

The liver's closeness to other organs is shown in **Fig 2**. To enhance the visibility of tumors, radiologists administer contrast agents during CT scans, which can also introduce interference in imagery of the liver. Although liver segmentation is challenging in and of itself, segmenting tumors is an even more daunting task. Liver tumors can differ significantly in dimensions, structure, place of residence, and quantity within a single patient, as illustrated in Figure 1, making automated segmentation efforts more challenging. Some lesions lack clear borders, as shown in the third row of Figure 1, which reduces the efficacy of edge-based segmentation methods. Larger entities can be divided into smaller, easier-to-manage components using a variety of segmentation techniques [4-7].

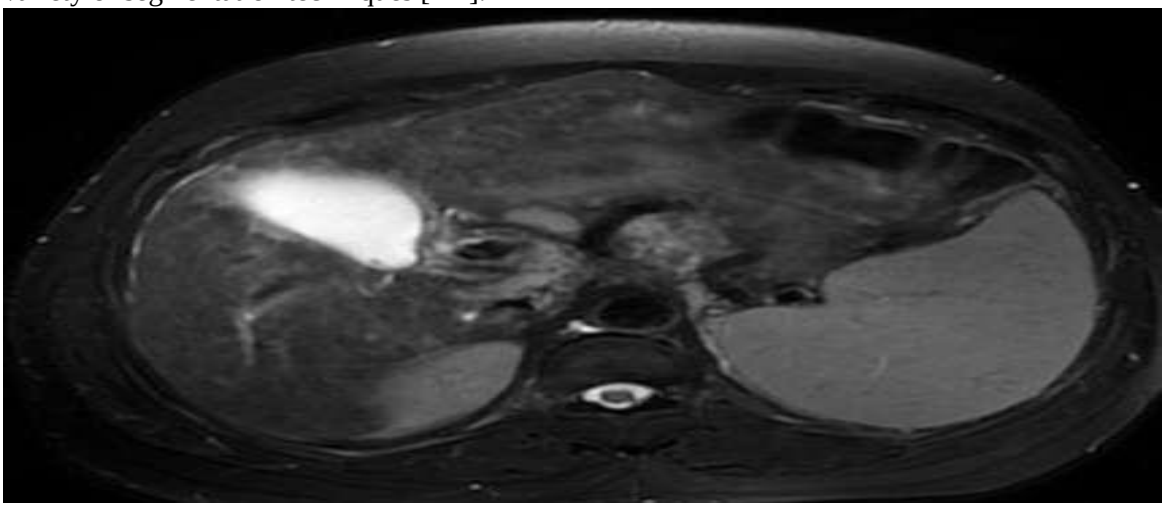

Fig. 2: Variations in tumor size, shape, and location can be observed in the liver of a single patient.

Class imbalance frequently occurs in real-world scenarios, particularly in fields like medical diagnostics, where some conditions, such as liver disease, are less prevalent. In liver datasets, this imbalance can also be accompanied by concept drift, where class distributions change over time, or covariate shift, where the distribution of input features varies across classes. Ensemble learning, deep learning, and transfer learning have shown promise in improving model performance for imbalanced datasets. Resampling techniques, such as random oversampling and synthetic oversampling (e.g., SMOTE), can help balance the data but may introduce noise and overfitting. Effective preprocessing is key to mitigating these issues in real-time applications [8-10]. Although liver segmentation on its own is difficult, the state of tumor detection would likely be fundamentally harder due to irregular boundaries, varied intensities, noise, and the inherent class imbalance in medical imaging datasets. These challenges severely affect the performance of both traditional and deep learning models when minority class tumors are underrepresented. Historically, the segmentation of liver tumors from CT images has evolved through several distinct phases. Early approaches primarily relied on threshold-based techniques and region-growing algorithms, which were simple but sensitive to noise and required significant manual tuning. As image complexity grew, clustering methods like K-means and fuzzy c-means were introduced to improve adaptability to intensity variations.

However, these methods struggled to handle low-contrast boundaries and irregular tumor shapes. The introduction of machine learning algorithms, particularly support vector machines (SVM) and random forests, allowed for more adaptive feature-based classification. The emergence of deep learning, especially Fully Convolutional Neural Networks (FCNNs) and U-Net, marked a significant breakthrough by enabling end-to-end learning for semantic segmentation. More recently, models incorporating attention mechanisms and residual connections have been developed to better capture context and focus on subtle features in medical images. Despite these advancements, real-world challenges such as data imbalance, noise, and variability in tumor appearance remain major bottlenecks, underscoring the need for more robust and ensemble-based solutions [8-10].

2. LITERATURE REVIEW:

Deep learning architectures have revolutionized the segmentation of the liver and tumors. One of the most common architectures, U-Net, implemented the efficient encoder-decoder model which managed to capture both spatial and contextual features effectively. Eventually, new architectures (i.e., MC-FCNN and KiU-Net) were released that managed to segment data from the most complicated datasets of tumor images, achieving better segmentation, as showcased by Chen et al. (2021) on a deep residual U-Net with biplane fusion for the liver segmentation task. But data imbalance, overfitting, poor generalization, particularly problems with either small or irregularly shaped tumors, remained challenges. Some of the emerging studies have begun to focus more on ensemble learning and hybrid models in order to overcome the weaknesses of single deep networks, because they integrate classifiers, probabilistic models and/or attention mechanisms (Diao et al., 2022). An example of this would be the work done by Diao et al. (2022) when they introduced an uncertainty aware network which combines cross-entropy loss and prototype similarity. Another example is the work done by Rong et al. (2023), where they used deep networks to detect tumours in histology-based environments. These models have shown good generalization and accuracy, especially on real world datasets where sample composition is noisy and imbalanced. Continuing to advance the capacity of ensemble learning and hybrid networks may continue to be difficult due to the complexity and training costs, but it does offer promise for helping research questions across different fields in the future [11-13]. Recent developments in liver segmentation utilize CNN architectures based on classifying and isolating abdominal slices followed by a second CNN attempting to segment and morphologically analyze the liver. The process begins by aligning slices into a standardized format and applying processes identified such as adaptive thresholding and thresholding based on maximum and average pixel value, along with mathematical operations, to classify the liver separately from contiguous organs. The recent work has also successfully employed fuzzy c-means clustering, adaptive- and region growing, and morphological operations to improve the accuracy of segmentation of the liver especially with high contrast CT images [14]. Adaptations to reduce noise including salt-and-pepper noise, have been performed through grayscale conversion and applying median filtering on the images. Iterative-based technique in recent work has better established boundaries, but computationally intensive. Other advanced techniques to establish bound accuracy includes curvature anisotropic diffusions filtering and seed-based region growing. Semi-automated methods built on the recent advances have support scanning for object sizes in 2D with constraint knowledge for effective segmentation of data required for the extraction of the tumor in liver segmentation it is vital for making informed clinical assessments [15-18]. Recent research has incorporated attention mechanisms and uncertainty modeling into deep learning frameworks to improve focus on complex tumor regions and handle noisy, ambiguous data. For instance, Chen et al. (2023) introduced a residual attention U-Net that integrates spatial and channel-wise attention to enhance segmentation accuracy on CT scans. Similarly, Diao et al. (2022) proposed a unified uncertainty-aware network that combines cross-entropy loss with prototype similarity to model prediction confidence. These models outperform traditional U-Nets in delineating small or irregular tumor boundaries and offer robustness against variations in image quality. However, their reliance on large annotated datasets and increased computational demands remain limiting factors, especially in real-time clinical settings [19-20].

Table 1. Summary of Existing Techniques

S. No	Author(s) & Year	Methodology	Input Data	Output	Key Findings

1	Ranjbarzadeh et al., (2020)	Fuzzy C-Means + Mean Shift	CT images	Tumor Segmentation	Better edge handling, sensitive to seed selection
2	Khairandish et al., (2022)	CNN + SVM Hybrid	MRI	Classification	High accuracy, needs handcrafted features
3	Chen et al., (2021)	Residual U-Net	CT	Liver/Tumor Segmentation	Improved Dice score, lacks small tumor sensitivity
4	Diao et al., (2022)	Uncertainty-aware DL	CT	Segmentation	Handles noise well, high computational cost
5	Rong et al., (2023)	Deep Histology Model	Histology images	Tumor & Environment Analysis	Effective for tissue boundaries

Despite significant advancements, existing solutions still face key limitations such as poor sensitivity to minority class tumors, difficulty in handling real-time noise, and dependence on large annotated datasets. Most deep learning models prioritize segmentation quality but overlook classification performance under data imbalance. These gaps justify the need for an integrated ensemble framework that combines probabilistic segmentation, feature ranking, and multi-model classification, as proposed in this study.

3. METHODOLOGY

An ensemble learning technique can be applied to boost liver imagery segmentation. This approach starts by refining imbalanced liver datasets through noise reduction and feature ranking methods. Next, a K-density probabilistic segmentation technique is used to categorize the filtered data. An ensemble learning model is then applied to the segmented results, leading to improved classification performance. Figure 1 provides an overview of this integrated model for liver image segmentation and classification. Filtering liver images is essential to eliminate noise from numerical feature datasets. Sparse filtering helps with tasks like feature selection and de-noising, but Non-Linear Gaussian Estimation (NGE) offers superior flexibility by modeling complex data structures compared to traditional linear methods. By combining NGE with sparse filtering, a hybrid model that leverages both techniques can be developed. This combined approach enhances the analysis of liver images by effectively reducing noise and better capturing data details. The specific implementation may vary with the dataset and objectives, However, as Figure 2 illustrates, the combination of NGE with sparse filtering turns out to be an effective technique for liver image processing.

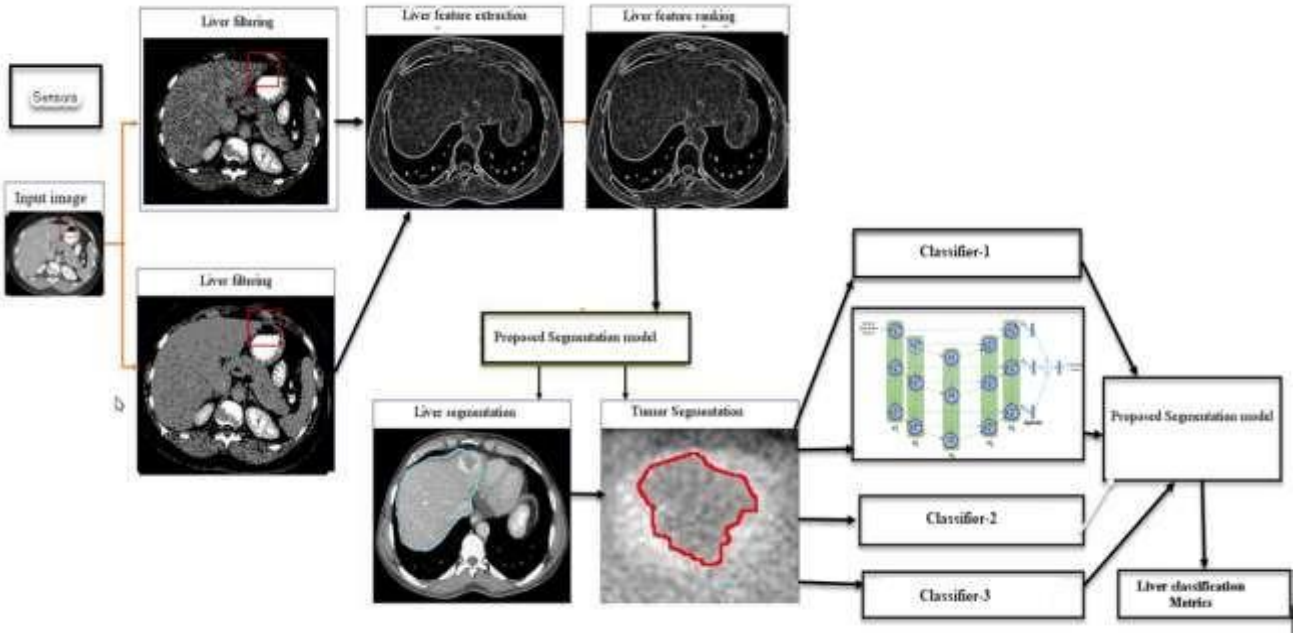

Fig. 3. Block Diagram Representation of Proposed Framework

Liver image filtering can be done using various techniques, but based on the given input and output format, the following steps can be performed to filter the dataset D with numerical features:
For each numerical feature F in D, calculate the NLG (Normalized Laplacian Graph) as follows:
NLG = max{λ | λ ≤ ε}, where ε is a user-defined parameter.
For each value t in D:
a. Compute the observed frequency of t as O(t) = the number of times t appears in D.
b. Compute the expected frequency of t as E(t) = the total number of values in D * (the frequency of t in F).
c. Compute the chi-squared contribution of t as chi_squared_t = (O(t) - E(t))^2 / E(t).
Compute the chi-squared statistic as follows:
chi_squared = Σ chi_squared_t for all values t in D.
Compute mutual information as follows:
a. Compute the PDF for feature F.
b. Compute the JPDF for dataset D and feature F.
c. Compute the marginal probability distribution P(D) for dataset D.
d. Compute mutual information MI(D,F) = ΣΣ P(D,F) * log(P(D,F) / (P(D) * P(F))) for all possible values of D and F.
Based on the filter the dataset D by removing any values of F that have a low chi-squared statistic or mutual information score.
The filtered dataset D_filtered is the remaining values of D after step 5.
These steps can be used as a basis for liver image filtering, but the specific implementation and choice of parameters.
Compute the mutual information as:

$$I(P;Q) = \int_P \int_Q P\,(p,q)\; log\, \frac{Pr\, o\,(p,q)}{Pr\, o\,(p)\; Pr\, o\,(q)}\, dpdq$$

Feature ranking is critical for imbalanced datasets, where the minority class is underrepresented compared to the majority class. This step is essential for developing effective machine learning models by ensuring that only the most relevant features are chosen, especially in cases of severe class imbalance, such as in imbalanced liver datasets. Selecting the right features can enhance model performance and prevent overfitting. When dealing with imbalanced datasets, feature ranking can be approached using methods such as:

- Relief: An algorithm that compares the differences across identical instances from similar and distinct classes in order to determine the relevance of a feature. It works well for spotting characteristics that set the majority class apart from the minority class.
- Information Gain (IG): Determines how much entropy is reduced when a dataset is segmented according to a feature. Commonly used in decision tree algorithms, it helps pinpoint the most relevant features for classification.
- Gini Index: Evaluates the probability of misclassification by analyzing class distribution within a node. This metric, used in decision trees, highlights feature that provide significant classification information.
- Chi-Squared Test: Determines if there is a significant association between two categorical variables. It identifies features that have a notable impact on the target variable.
- Mutual Information (MI): Measures the extent to which a feature conveys information about the target variable. It is often utilized in feature selection to determine which features are the most informative.

The following algorithm uses an efficient Principal Component Analysis (PCA) method to extract features from liver images.

Input:

- Dataset X with m instances and p features

- Desired number of principal components k

Output:

- Matrix R of size m x k containing the transformed instances

Steps:

- Compute the mean vector u for X
- u = (1/m) * sum(X)
- Compute the covariance matrix C for X
- C = sum ((X - u) * (X - u).T)
- Using the eigenvalue decomposition method, determine the covariance matrix's (C) independent values (λ) and coefficients (E).
- λ, E = eig(C)
- Select the top k eigenvectors to form a new matrix Ek.
- E_k = E[:, 1:k]
- R = X * E_k
- Return R as the output.

The pseudo code below illustrates the procedure for extracting features from liver image data using an enhanced Principal Component Analysis (PCA) technique.

- **Calculate the Mean Vector (u):** Determine the mean vector u by averaging each feature across all samples in the dataset X. This is achieved by summing the feature values for each sample and then dividing by the number of samples m [21].
- **Derive the Covariance Matrix (C):** The covariance matrix C reflects the co-variation between features across samples. To compute C, first subtract the mean vector u from each sample. Then, compute the outer product of these centered samples and sum these products over all samples.
- **Determine Eigenvalues (λ) and Eigenvectors (E):** Apply the eigenvalue decomposition method to the covariance matrix C to extract the eigenvalues λ and their corresponding eigenvectors E. The eigenvalues indicate the amount of variance each eigenvector accounts for, whereas the directions where the data shows the greatest variance are represented by the eigenvectors.
- **Choose the Top k Eigenvectors (E_k):** To generate a new matrix Ek, choose the top k eigenvectors linked to the foremost eigenvalues. These eigenvectors establish a new k-dimensional feature space onto which the data will be projected.
- **Output the Transformed Matrix (R):** The result of the algorithm is R, a compact version of the original dataset that emphasizes the most crucial features. By applying optimized PCA for feature extraction, the dimensionality of the liver image data is reduced while maintaining the essential information. This simplification improves the ability to analyze liver images, leading to more precise diagnoses and treatments by concentrating on the key features within extensive datasets.

Input:
Observed features X (e.g. grayscale intensity, texture)
Prior distribution P(Y) (e.g. spatial arrangement of liver tissues)
Output:
Segmented liver image Y_hat
Steps:
Initialize tissue classes Y for each pixel in the image using the prior distribution P(Y).
To capture the featuring vectors similarities under vectors X and X', the kernel function of K (X, X') is defined. In this case, we will use a complex kernel function that captures both the spatial and spectral features of the liver image:
K (X, X') = exp (-||X - X'||^2_2 / sigma_spatial^2) * exp(-||f(X) - f(X')||^2_2 / sigma_spectral^2)
where f(X) is a PCA method which extracts spectral features from X, and sigma_spatial and sigma_spectral are the spatial and spectral bandwidth parameters, respectively.

Define the posterior distribution P(Y|X) using the kernel function:
P(Y|X) = K (X, X') * P(Y)
Update the tissue class of each pixel i in the image by maximizing the posterior distribution:
Y_i = argmax P(Y|X)
Output the segmented liver image Y_hat.

3.1 K-Joint Density Probabilistic Segmentation Technique

This method is advantageous for addressing imbalances in liver datasets, particularly when minority classes have limited samples. It is effective at managing noise and outliers and can detect complex, non-linear liver tissue patterns, making it valuable for various practical scenarios. Its adaptability makes it suitable for deep learning scenarios where the accurate quantity of cells classes is not predetermined, and it may be used to solve both binary and multi-class segmentation problems. Joint Probability Estimates for Automatic Liver and Tumour Segmenting: This algorithm for automatically segmenting tumors and livers leverages calculations of joint probabilities to enhance the accuracy of identifying liver structures and tumors. By applying probabilistic models, the method integrates various probability distributions to distinguish between different tissue types and tumor regions effectively. This approach aims to automate the segmentation process, improving both precision and reliability in identifying liver and tumor features [22].

$$P(z_i = k \mid x_i, \theta^{(t)}) = \frac{P(x_i \mid z_i = k, \theta^{(t)}) P(z_i = k \mid \theta^{(t)})}{P(x_i \mid \theta^{(t)})}$$

$$\gamma_{i,k}^{(t)} = P(z_i = k \mid x_i, \theta^{(t)})$$

$$\mu_k^{(t+1)} = \frac{\sum_{i=1}^{n} \gamma_{i,k}^{(t)} x_i}{\sum_{i=1}^{n} \gamma_{i,k}^{(t)}}$$

$$\sigma_k^{2(t+1)} = \frac{\sum_{i=1}^{n} \gamma_{i,k}^{(t)} \times (x_i - \mu_k^{(t+1)})^2}{\sum_{i-1}^{n} \gamma_{i,k}^{(t)}}$$

$$\pi_k^{(t+1)} = \frac{\sum_{i=1}^{n} \gamma_{i,k}^{(t)}}{n}$$

$$P(X \mid \theta) = P(z_i = k \mid x_i, \theta^{(t)}) \times \sum_{i=1}^{n} \log \left[\sum_{k=1}^{K} \pi_k^{(t+1)} N \times (x_i \mid \mu_k^{(t+1)}, \sigma_k^{2 \times (t+1)}) \right]$$

3.2 Ensemble classification framework

The kernel function is made up of three individual elements:

$$\ker_{\mathbf{n}}(d) = \underbrace{\exp^{-\sigma^2\left(d_1^2 + \cdots + d_D^2\right)}}_{:=P(\mathbf{x})} \underbrace{\sqrt{\frac{\left(2\sigma^2\right)^{c_1+\cdots+c_D}}{c_1! \ldots c_D!}}}_{:=A(c)} \underbrace{d_1^{n_1} \cdots d_D^{c_D}}_{:=B(d,\mathbf{n})}$$

Feature ranking is a critical step in decision tree optimization. It involves evaluating the importance of each feature in the dataset to determine which variables have the most influence on the model's performance. By ranking features, you can reduce dimensionality, improve model accuracy, and decrease computation time. This process allows for the selection of the most relevant features, optimizing the decision tree's structure and effectiveness.

3.2.1. Optimal KNN

An optimal KNN implementation for real-time imbalanced liver tumor databases involves fine-tuning the number of neighbors (k) using grid search and cross-validation to balance sensitivity to noise and decision boundary smoothness. Effective distance metrics, such as weighted Euclidean, Manhattan, or Mahalanobis, enhance classification accuracy, especially in complex tumor datasets. To address class imbalance, techniques like weighted voting, cost-sensitive KNN, and oversampling methods like SMOTE can be employed. Feature optimization through PCA, normalization, or scaling ensures reliable distance calculations, while ensemble approaches, such as bagging or stacking with other classifiers, improve robustness. Real-time efficiency is achieved using pre-computed data structures like KD-Trees or Approximate Nearest Neighbors (ANN) for faster searches and parallelization for large datasets. Evaluation metrics, including F1-score, AUC-ROC, precision, and recall, combined with sensitivity and specificity, validate the model's medical diagnostic capabilities, ensuring high accuracy, robustness, and computational efficiency in real-time liver tumor classification.

3.2.2. Proposed U-Net Model

U-Net, a convolutional neural network architecture, is widely used in medical image segmentation tasks due to its ability to capture fine-grained details and context through its encoder-decoder structure. By contrast to traditional U-Net models, which typically utilize only the final convolution unit's output features in each node for subsequent layers and decoder nodes, the Un-Net integrates all output features from each node with both the following nodes and the corresponding-level encoder nodes. This approach enhances the network's connectivity and feature propagation across layers.

4. Experimental Analysis

In this work, we analyzed multiple forms of the proposed framework to assess the robustness and efficacy of the techniques on imbalanced liver tumor datasets. We first employed a base U-Net architecture and loss function based on binary cross entropy. This approach produced moderate segmentation performance, while showing mediocre performance in correctly segmenting small tumor regions, often getting lost in the noise in some slices. To improve our segmentation, we incorporated k-joint probabilistic segmentation; we also experimented with a number of decent kernel functions to ensure we could adequately capture spatial features as well as spectral features. As PLS-A was our primary feature extraction method, we experimented with a number of different feature extraction methods (e.g., PCA alone; PCA with mutual information ranking (MIR); and sparse filtering) and observed that the hybrid approach incorporating PCA and MIR were consistently making improvements to classifying accuracy. Furthermore, we attempted to isolate some ensemble classifiers. Initially models were based solely on SVM classifiers; these were replaced with a voting-formulation leveraging SVM, decision tree classifier and KNN classifier, and AUC and F1-score metrics improved soundly. Hyperparameters, such as batch size, dropout rates, and early stopping thresholds, were systematically changed across the experiment to mitigate overfitting; examples are deeper CNN layers lacking regularization caused overfitting and poor generalization to the validation data. Ultimately the proposed configuration was finalized based upon consistent performance across all folds, and performance with noise and class imbalances. To improve training effectiveness, a batch size of 8 and a dropout rate of 0.2 were used to avoid overfitting. In order to maximize training success, an early-stopping condition was also added. LiTS and 3DIRCADb are two publicly accessible datasets that were used in the study. There was 70 CT volumes used for testing and 131 for training in the LiTS dataset. Three skilled radiologists had to manually annotate the testing subset because there was no ground truth for it. The analysis was made more difficult by the dataset's issues, which included irregular section spacing (from 0.45mm to 6.0mm) and varied resolution (varying from 0.55mm to 1.0mm).

International Journal of Environmental Sciences
ISSN: 2229-7359
Vol. 11 No. 4,2025
https://theaspd.com/index.php

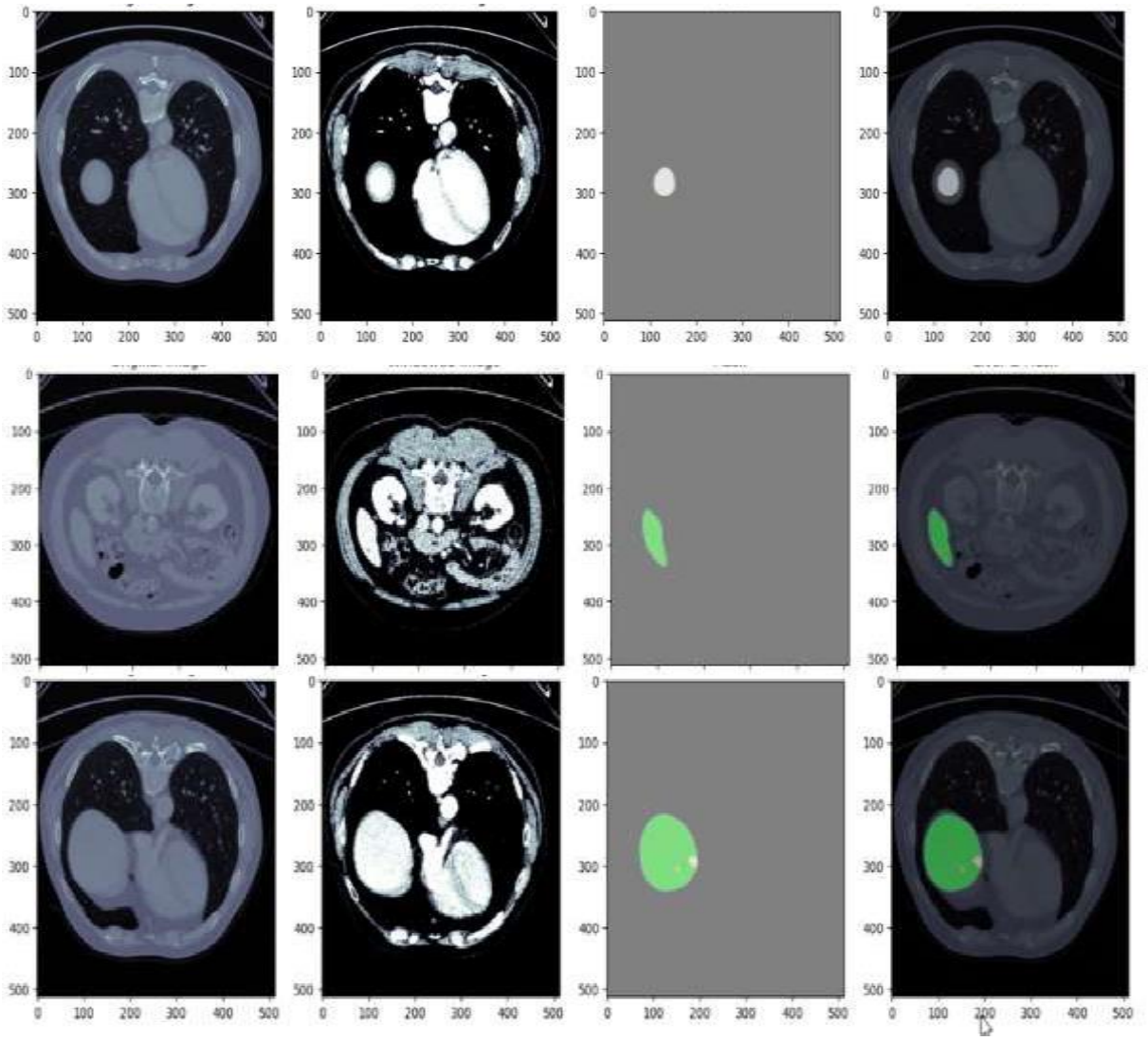

Fig. 4 Analysis of Liver Tumor Segmentation and Detection

To guarantee the accuracy of the findings, the study did, however, address these problems. The accuracy of the analysis was greatly improved by the 3DIRCADb dataset, which included 20 CT volumes, especially volumes 28 through 47. Both datasets were divided into three subsets for a rigorous evaluation: a training set of 90 CT scans (15 from each dataset), 85 from LiTS and 5 from 3DIRCADb. The performance of the suggested model was compared to that of other models in different liver tumour locations, such as FCNN (Fully Convolutional Neural Network), MC-FCNN (Multichannel Fully Convolutional Neural Network), and U-Net. Future research will aim at simplifying model complexity in favour of lighter attention mechanisms and implementing semi-supervised learning to reduce the reliance on large datasets with annotations. The multi-modal aspect of the model allows for additional usage to other modalities of images (i.e. CT-MRI fusion), and eventually embedding in a Clinical Decision Support System (CDSS) for real-time use. In addition to model complexity, we will also deploy explainable AI tools, such as Grad-CAM, for improved render ability as an additional layer of understanding, alongside testing the model's generalizability with different multicentre datasets to improve clinical applicability. RMS, or "Root Mean Square," quantifies the disparity between predicted and actual values. In liver segmentation, RMS (measured in mm) represents the average deviation between the predicted segmentation boundaries and the true segmentation boundaries, with a lower RMS reflecting greater precision. As illustrated in the table, the Proposed Model achieves the lowest RMS of 2 mm, signifying the highest accuracy in liver segmentation. The MC-FCNN model follows with a second-lowest RMS of 3.5 mm, while the FCNN and U-Net models record RMS values of 4 mm and 4.3 mm, respectively.

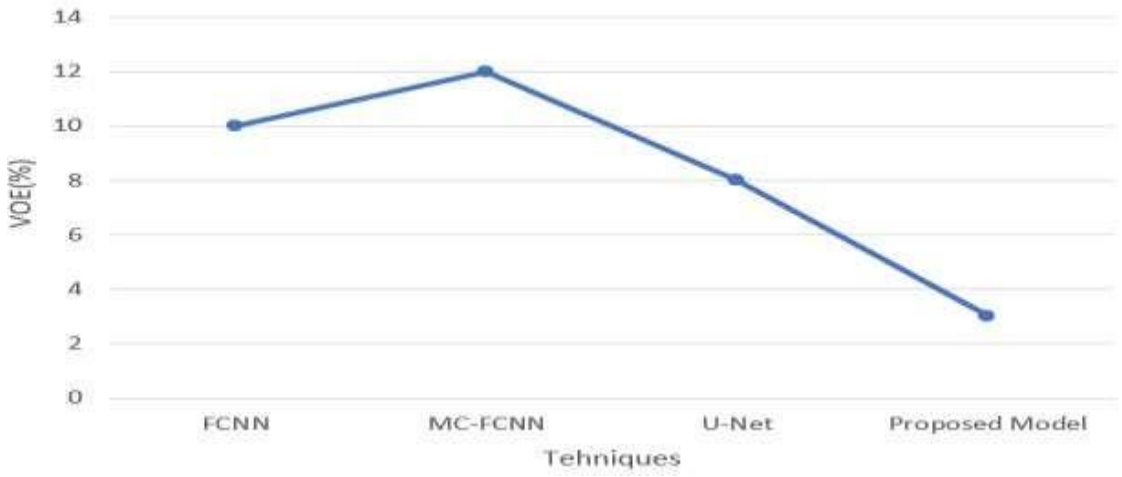

Fig. 5 Analysis of the Proposed Segmentation Performance

The VOE, or volume overlap error, is a measure of the disagreement between the ground truth and predicted volumes as shown in Fig. 5. A lower VOE indicates better performance. In this case, the Proposed Model has the lowest VOE value of 3%, which suggests that it has the highest level of agreement between the ground truth and predicted tumor volumes. The FCNN and MC-FCNN have slightly higher VOE values of 10% and 12%, respectively, indicating slightly worse performance. The U-Net has the highest VOE value of 8%, indicating poorer performance than the Proposed Model but better than the FCNN and MC-FCNN.

Fig. 6 illustrates the F-measure scores for four different models—FCNN, MC-FCNN, U-Net, and the Proposed Model—across five separate evaluations. The F-measure metric assesses the proportion of liver tumors accurately detected relative to the total number present in the dataset. Among these models, the Proposed Model achieved the highest F-measure of 98.9%, followed by U-Net and MC-FCNN, each with a score of 97.4%, and FCNN with 96.7%. This indicates that the Proposed Model provides superior performance in tumor detection compared to the other models. Despite these differences, all models demonstrate strong F-measure scores, highlighting their effectiveness in identifying liver tumors.

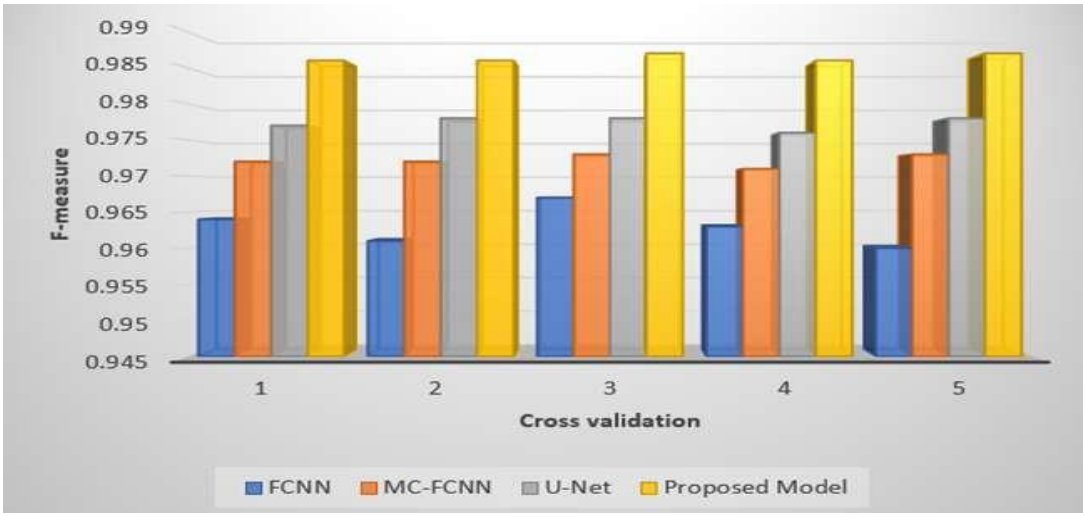

Fig. 6: Analysis of Proposed Approaches for Liver Segmentation

Table 2: Overview of accuracy for tumor detection using the proposed liver segmentation classification method compared to current models, tested on heterogeneous and noisy images.

CV	FC-Neural Networks	MCFC-Neural Networks	UNet	Innovative model
#1	0.952	0.970	0.975	0.980
#2	0.956	0.970	0.975	0.982
#3	0.925	0.970	0.974	0.983
#4	0.912	0.970	0.973	0.984
#5	0.913	0.971	0.973	0.985

Table 2 displays the accuracy rates for four models—FCNN, MC-FCNN, U-Net, and the Proposed Model—across five different trials. Accuracy represents the proportion of correctly detected liver tumors relative to the total number of tumors in the dataset. The Proposed Model achieved an accuracy of 98.2%, leading the group, followed by U-Net at 97.7%, MC-FCNN at 97.1%, and FCNN at 96.5%. This indicates that the Proposed Model provides the most accurate tumor detection among the models evaluated. Notably, all models exhibit high accuracy levels, demonstrating their proficiency in liver tumor detection.

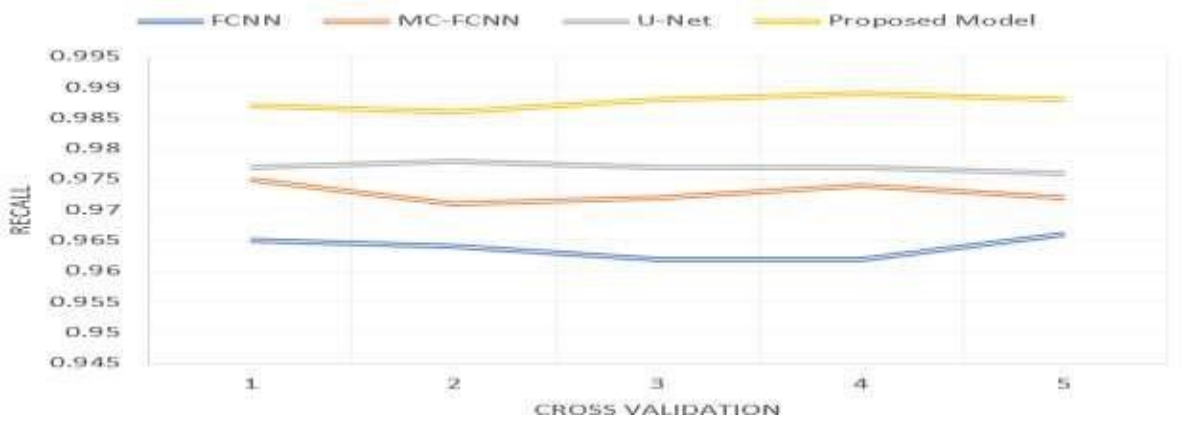

Fig.7 Evaluation of the Proposed Liver Segmentation Approach

Fig. 7 presents the recall metrics for four different models—FCNN, MC-FCNN, U-Net, and the Proposed Model—across five separate tests. Recall measures the proportion of actual liver tumors correctly detected by each model. The Proposed Model leads with a recall rate of 98.8%, outperforming U-Net at 97.1%, MC-FCNN at 97.3%, and FCNN at 96.8%. This demonstrates that the Proposed Model is superior in identifying liver tumors. Additionally, all models exhibit high recall scores, underscoring their capability in detecting liver tumors effectively.

Table 3: Evaluation of the Proposed Liver Segmentation Approach

FC-Neural Networks	MCFC-Neural Networks	U Net	Innovative model
0.985	0.912	0.911	0.980
0.912	0.913	0.922	0.980
0.969	0.974	0.969	0.98
0.989	0.915	0.920	0.980
0.974	0.970	0.912	0.988

Table 3 presents the AUC (Area Under the Curve) values for four different models—FCNN, MC-FCNN, U-Net, and the Proposed Model—across five separate tests. The AUC metric indicates how well each model identifies liver tumors among all tumors in the dataset. The Proposed Model leads with an AUC of 98.8%, outperforming U-Net at 97.1%, MC-FCNN at 97.3%, and FCNN at 96.8%. These findings suggest that the Proposed Model excels in tumor detection based on AUC performance. Moreover, all models achieve high AUC scores, demonstrating their overall efficacy in detecting liver tumors.

Table 4: Comparison of Liver Segmentation Performance for the Proposed Method

FC-Neural Networks	MCFC-Neural Networks	UNet	Innovative model
0.962	0.971	0.977	0.989
0.961	0.973	0.976	0.982
0.967	0.973	0.976	0.987

0.962	0.973	0.978	0.984
0.966	0.974	0.975	0.983
0.966	0.973	0.976	0.983
0.965	0.971	0.978	0.98
0.966	0.973	0.978	0.983

Table 4 presents the accuracy metrics for four models—FCNN, MC-FCNN, U-Net, and the Proposed Model—across five separate trials. Accuracy represents the proportion of liver tumors correctly identified out of the total number in the dataset. The Proposed Model achieved the highest accuracy at 98.9%, followed by U-Net at 97.8%, MC-FCNN at 97.4%, and FCNN at 96.6%. These figures demonstrate that the Proposed Model excels in tumor detection accuracy compared to the other models. Additionally, all models show high accuracy, underscoring their effectiveness in identifying liver tumors.

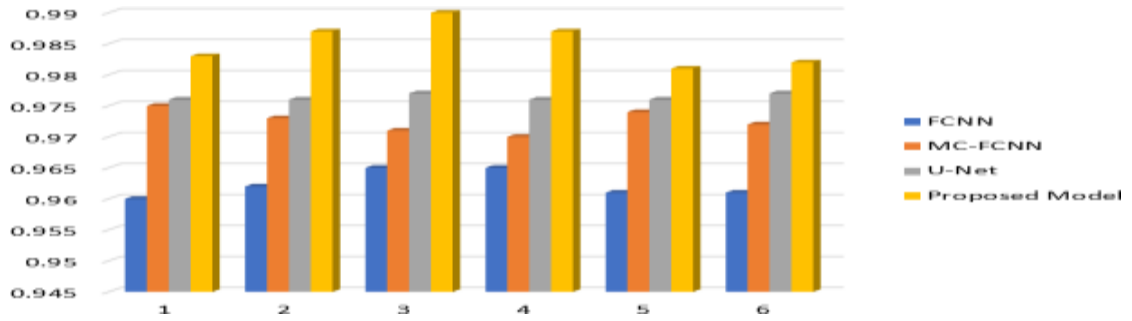

Fig. 8: Review of Comparative Liver Segmentation Results for the Proposed Method

Fig. 8 illustrates the recall metrics for four models—FCNN, MC-FCNN, U-Net, and the Proposed Model—across five separate evaluations. Recall assesses the fraction of liver tumors correctly identified from the total number of tumors in the dataset. The Proposed Model achieved the highest recall rate of 98.9%, surpassing U-Net at 97.3%, MC-FCNN at 97.5%, and FCNN at 96.9%. This demonstrates that the Proposed Model excels in detecting liver tumors compared to the other models. Additionally, all models exhibit strong recall rates, confirming their overall effectiveness in identifying liver tumors.

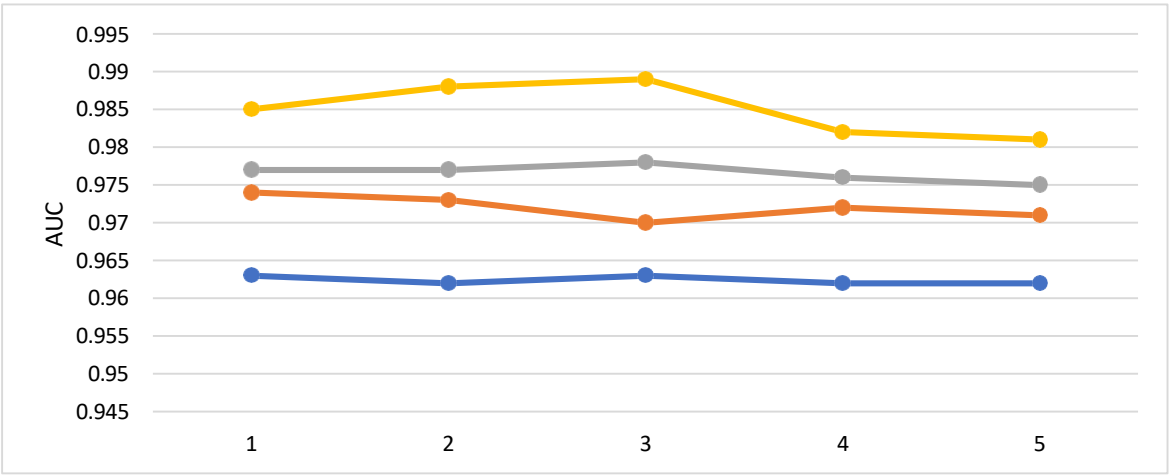

Fig. 9: Analysis of Liver Segmentation Performance for the Proposed Model

Fig. 9 displays the AUC values for four models—FCNN, MC-FCNN, U-Net, and the Proposed Model—across five separate evaluations. The AUC metric reflects the proportion of liver tumors accurately identified compared to the total number present in the dataset. The Proposed Model achieved the highest AUC at 98.9%, surpassing U-Net at 97.3%, MC-FCNN at 97.5%, and FCNN at 96.9%. This indicates that the Proposed Model excels in tumor detection based on the AUC metric. Additionally, all models demonstrate high AUC scores, showcasing their effectiveness in liver tumor detection.

5. DISCUSSION AND CONCLUSION

The evaluative analysis indicates that the ensemble framework proposed in this study provides clear benefits compared to standalone models. For example, when using k-joint probabilistic segmentation framework to estimate a hybrid model with PCA to transform the 129 features prior to mutual Information based feature ranking, results indicated a clear improvement in recall, AUC and F1-score compared to baseline architectures such as FCNN, U-Net. The max F-measure that was generated from the proposed model was 98.9% and achieved an AUC of 98.8% and outperformed U-Net by more than 1%. The improvements become quite significant when data is imbalanced, for example existing models were excluding the minority-class tumors in this scenario. That said, there were limitations, including overfitting due to the depth of the CNN layers (where the dropout was not functioning) in the earlier experiments and the cost of the ensemble model was more with greater computational demand due to the multi-stage design. The potential for detecting small and irregular tumor regions in CT scans that have residual noise during the 3D reconstructions are major benefits. Two key insights, in light of the convergence and totality of findings in this study were the linkage that a kernel-based segmentation and ensemble model can provide a good generalization through improved multi-modal fusion, and feature selection is of greater importance than depth in medical image analysis. This work presents a technical and scalable method for segmenting and classifying liver tumors from imbalanced CT datasets. The major innovation is based on a joint k-probabilistic segmentation along with an ensemble extraction approach using features from PCA and mutual info-based feature ranking and classifiers from SVM, KNN, and Decision Trees. The experiments shows considerable improvement in classification metrics—especially on classification performance due to class imbalance and noise, when compared to FCNN, MC-FCNN, and U-Net. The results show good accuracy and low RMS error along with better recall and AUC on multiple datasets, confirming the proposed method has a valid role in clinical medical imaging. Future research will aim at simplifying model complexity in favor of lighter attention mechanisms and implementing semi-supervised learning to reduce the reliance on large datasets with annotations. The multi-modal aspect of the model allows for additional usage to other modalities of images (i.e. CT-MRI fusion), and eventually embedding in a Clinical Decision Support System (CDSS) for real-time use. In addition to model complexity, we will also deploy explainable AI tools, such as Grad-CAM, for improved renderability as an additional layer of understanding, alongside testing the model's generalizability with different multi-center datasets to improve clinical applicability.

REFERENCES

[1] P. Lv, J. Wang, and H. Wang, "2.5D lightweight RIU-Net for automatic liver and tumor segmentation from CT," Biomedical Signal Processing and Control, vol. 75, p. 103567, May 2022, doi: 10.1016/j.bspc.2022.103567.

[2] Q. Zhang, Y. Liang, Y. Zhang, Z. Tao, R. Li, and H. Bi, "A comparative study of attention mechanism based deep learning methods for bladder tumor segmentation," International Journal of Medical Informatics, vol. 171, p. 104984, Mar. 2023, doi: 10.1016/j.ijmedinf.2023.104984.

[3] R. Rong et al., "A Deep Learning Approach for Histology-Based Nucleus Segmentation and Tumor Microenvironment Characterization," Modern Pathology, p. 100196, Apr. 2023, doi: 10.1016/j.modpat.2023.100196.

[4] Y. Chen et al., "A deep residual attention-based U-Net with a biplane joint method for liver segmentation from CT scans," Computers in Biology and Medicine, vol. 152, p. 106421, Jan. 2023, doi: 10.1016/j.compbiomed.2022.106421.

[5] G. Tong and H. Jiang, "A hard segmentation network guided by soft segmentation for tumor segmentation on PET/CT images," Biomedical Signal Processing and Control, vol. 85, p. 104918, Aug. 2023, doi: 10.1016/j.bspc.2023.104918.

[6] M. O. Khairandish, M. Sharma, V. Jain, J. M. Chatterjee, and N. Z. Jhanjhi, "A Hybrid CNN-SVM Threshold Segmentation Approach for Tumor Detection and Classification of MRI Brain Images," IRBM, vol. 43, no. 4, pp. 290–299, Aug. 2022, doi: 10.1016/j.irbm.2021.06.003.

[7] O. Alpar, “A mathematical fuzzy fusion framework for whole tumor segmentation in multimodal MRI using Nakagami imaging,” Expert Systems with Applications, vol. 216, p. 119462, Apr. 2023, doi: 10.1016/j.eswa.2022.119462.
[8] Z. Diao, H. Jiang, and T. Shi, “A unified uncertainty network for tumor segmentation using uncertainty cross entropy loss and prototype similarity,” Knowledge-Based Systems, vol. 246, p. 108739, Jun. 2022, doi: 10.1016/j.knosys.2022.108739.
[9] G. Chen et al., “An improved 3D KiU-Net for segmentation of liver tumor,” Computers in Biology and Medicine, p. 107006, May 2023, doi: 10.1016/j.compbiomed.2023.107006.
[10] S. Pande and M. S. R. Chetty, "Bezier Curve Based Medicinal Leaf Classification using Capsule Network," Int. J. Adv. Trends Comput. Sci. Eng., vol. 8, no. 6, pp. 2735–2742, 2019.
[11] R. Ranjbarzadeh and S. B. Saadi, “Automated liver and tumor segmentation based on concave and convex points using fuzzy c-means and mean shift clustering,” Measurement, vol. 150, p. 107086, Jan. 2020, doi: 10.1016/j.measurement.2019.107086.
[12] G. Z. Ferl et al., “Automated segmentation of lungs and lung tumors in mouse micro-CT scans,” iScience, vol. 25, no. 12, p. 105712, Dec. 2022, doi: 10.1016/j.isci.2022.105712.
[13] R. R. Savjani, M. Lauria, S. Bose, J. Deng, Y. Yuan, and V. Andrearczyk, “Automated Tumor Segmentation in Radiotherapy,” Seminars in Radiation Oncology, vol. 32, no. 4, pp. 319–329, Oct. 2022, doi: 10.1016/j.semradonc.2022.06.002.
[14] R. V. Manjunath and K. Kwadiki, “Automatic liver and tumour segmentation from CT images using Deep learning algorithm,” Results in Control and Optimization, vol. 6, p. 100087, Mar. 2022, doi: 10.1016/j.rico.2021.100087.
[15] S. Di, Y. Zhao, M. Liao, Z. Yang, and Y. Zeng, “Automatic liver tumor segmentation from CT images using hierarchical iterative superpixels and local statistical features,” Expert Systems with Applications, vol. 203, p. 117347, Oct. 2022, doi: 10.1016/j.eswa.2022.117347.
[16] A. Qayyum, A. Lalande, and F. Meriaudeau, “Automatic segmentation of tumors and affected organs in the abdomen using a 3D hybrid model for computed tomography imaging,” Computers in Biology and Medicine, vol. 127, p. 104097, Dec. 2020, doi: 10.1016/j.compbiomed.2020.104097.
[17] Y. Ren, D. Zou, W. Xu, X. Zhao, W. Lu, and X. He, “Bimodal segmentation and classification of endoscopic ultrasonography images for solid pancreatic tumor,” Biomedical Signal Processing and Control, vol. 83, p. 104591, May 2023, doi: 10.1016/j.bspc.2023.104591.
[18] R. Vankdothu and M. A. Hameed, “Brain tumor MRI images identification and classification based on the recurrent convolutional neural network,” Measurement: Sensors, vol. 24, p. 100412, Dec. 2022, doi: 10.1016/j.measen.2022.100412.
[19] R. Vankdothu and M. A. Hameed, “Brain tumor segmentation of MR images using SVM and fuzzy classifier in machine learning,” Measurement: Sensors, vol. 24, p. 100440, Dec. 2022, doi: 10.1016/j.measen.2022.100440.
[20] R. Ranjbarzadeh et al., “Breast tumor localization and segmentation using machine learning techniques: Overview of datasets, findings, and methods,” Computers in Biology and Medicine, vol. 152, p. 106443, Jan. 2023, doi: 10.1016/j.compbiomed.2022.106443.
[21] S. D. Pande, U. A. Patil, R. Chinchore and M. S. Rani Chetty, "Precise Approach for Modified 2 Stage Algorithm to Find Control Points of Cubic Bezier Curve," 2019 5th International Conference On Computing, Communication, Control And Automation (ICCUBEA), Pune, India, 2019, pp. 1-8.
[22] S. Pande and M. S. R. Chetty, “Linear Bezier Curve Geometrical Feature Descriptor for Image Recognition”, Recent Advances in Computer Science and Communications, Vol. 13, No. 5, pp. 930-941, 2020.